

## Analytic Map of Three-Channel S Matrix: Generalized Uniformization and Mittag-Leffler Expansion


Wren A. Yamada<sup>1,2,\*</sup>, Osamu Morimatsu<sup>1,2,3,†</sup> and Toru Sato<sup>4,‡</sup>

<sup>1</sup>*Department of Physics, Faculty of Science, University of Tokyo, 7-3-1 Hongo Bunkyo-ku Tokyo 113-0033, Japan*

<sup>2</sup>*Theory Center, Institute of Particle and Nuclear Studies (IPNS), High Energy Accelerator Research Organization (KEK), 1-1 Oho, Tsukuba, Ibaraki 205-0801, Japan*

<sup>3</sup>*Department of Particle and Nuclear Studies, Graduate University for Advanced Studies (SOKENDAI), 1-1 Oho, Tsukuba, Ibaraki 305-0801, Japan*

<sup>4</sup>*Research Center for Nuclear Physics (RCNP), Osaka University, Ibaraki, Osaka 567-0047, Japan*

 (Received 1 April 2022; revised 15 July 2022; accepted 3 October 2022; published 31 October 2022)

We explore the analytic structure of the three-channel S matrix by generalizing uniformization and making a single-valued map for the three-channel S matrix. First, by means of the inverse Jacobi's elliptic function we construct a transformation from eight Riemann sheets of the center-of-mass energy complex plane onto a torus, on which the three-channel S matrix is represented single-valued. Second, we show that the Mittag-Leffler expansion, a pole expansion, of the three-channel scattering amplitude includes not only topologically trivial but also nontrivial contributions and is given by the Weierstrass zeta function. Finally, taking a simple nonrelativistic effective field theory with contact interaction for the  $S = -2$ ,  $I = 0$ ,  $J^P = 0^+$ ,  $\Lambda\Lambda - N\Xi - \Sigma\Sigma$  coupled-channel scattering, we demonstrate that as a function of the uniformization variable the scattering amplitude is, in fact, given by the Mittag-Leffler expansion and is dominated by contributions from neighboring poles.

DOI: [10.1103/PhysRevLett.129.192001](https://doi.org/10.1103/PhysRevLett.129.192001)

The spectrum of excited states and their structure are the central issues in the study of interacting quantum systems such as nuclear, hadron, atomic, and molecular systems. Those excited states show up as resonances embedded in the continuum spectrum. Extraction of resonance information from the continuum spectrum is one of the key subjects.

In hadron physics, many candidates of exotic hadrons have recently been found near the threshold of new hadronic channels [1,2]. However, most of the existing analyses of the spectra for these signals are unsatisfactory. For instance some assume the Breit-Wigner formula near the threshold, which cannot be justified, and/or an arbitrary background, while some others depend on particular models.

Very recently, a new method, the uniformized Mittag-Leffler expansion, has been proposed in Ref. [3] for extracting resonance information from the continuum spectrum. The method is theoretically well-grounded, model-independent, simple, and useful. The idea of the method is to find a variable in terms of which the S matrix is

single-valued (uniformization [4,5]) and to express the S matrix as a sum of pole terms (Mittag-Leffler expansion [6,7]). Therefore, it is crucial to find an appropriate uniformization variable that matches the analytic structure of the S matrix.

For the single-channel S matrix, the center-of-mass momentum serves a role as the uniformization variable, and the Mittag-Leffler expansion has already been studied in Refs. [8,9].

For the two-channel S matrix, a uniformization variable was introduced in Refs. [5,10] and the uniformized Mittag-Leffler expansion has been examined in the past few years [3,11,12].

Clearly, an extension of the method to three-channel reactions is an important step for the analysis of multi-channel scattering. Up to now, there have only existed some works in which an approximated local uniformization has been employed for the analysis of three-channel scattering [13–15]. It has been pointed out that the three-channel S matrix can be topologically mapped on a torus [5,16]. However, as far as we know, an explicit formula of the uniformization variable for the three-channel S matrix is yet to be known.

The purpose of this Letter is threefold. The first is to generalize uniformization. For the first time, we explicitly construct a uniformization variable for the three-channel S matrix. The second is to obtain an explicit expression of the Mittag-Leffler expansion for the three-channel scattering

---

*Published by the American Physical Society under the terms of the Creative Commons Attribution 4.0 International license. Further distribution of this work must maintain attribution to the author(s) and the published article's title, journal citation, and DOI. Funded by SCOAP<sup>3</sup>.*

amplitude taking account of both topologically trivial and nontrivial contributions. The third is to demonstrate the validity of the obtained results in a simple three-channel model.

Throughout this Letter, we assume that the singularities of the three-channel S matrix are poles and the three right-hand cuts starting from each threshold. We do not consider left-hand cuts or other singularities that cannot be removed by the present uniformization.

First, we generalize uniformization to the three-channel S matrix. As a function of  $\sqrt{s}$ , the Riemann surface for a three-channel S matrix is an eight-sheeted complex plane with three branch points at  $\sqrt{s} = \varepsilon_1, \varepsilon_2, \text{ and } \varepsilon_3$  ( $\varepsilon_1 < \varepsilon_2 < \varepsilon_3$ ), where  $\varepsilon_i = M_i + M'_i$  is the threshold energy,  $M_i$  and  $M'_i$  are the masses of particles in the  $i$ th channel. We also define ‘‘momentum,’’  $q_i = \sqrt{s - \varepsilon_i^2}$  and  $\Delta_{ij}$  by  $\Delta_{ij} = \sqrt{\varepsilon_j^2 - \varepsilon_i^2}$  for later use. The center-of-mass momentum,  $k_i$ , is given by  $\sqrt{s} = \sqrt{M_i^2 + k_i^2} + \sqrt{M_i'^2 + k_i^2}$ .  $q_i$  coincides with  $k_i$  up to a factor of 2,  $q_i = 2k_i$ , only when  $M_i = M'_i$ .

The uniformization of the three-channel S matrix is carried out in two steps. We uniformize channels 1 and 2 in the first step and channel 3 in the second step.

The first step is the same as the uniformization of the two-channel S matrix for channels 1 and 2 [5,10]. We define  $z_{12}$  by

$$z_{12} = \frac{q_1 + q_2}{\Delta_{12}}. \quad (1)$$

Inversely,  $q_1$  and  $q_2$  are given as single-valued functions of  $z_{12}$  by

$$q_1 = \frac{\Delta_{12}}{2} \left( z_{12} + \frac{1}{z_{12}} \right), \quad q_2 = \frac{\Delta_{12}}{2} \left( z_{12} - \frac{1}{z_{12}} \right). \quad (2)$$

$q_3$  is given by

$$q_3 = \frac{\Delta_{12}}{2} z_{12} \sqrt{\left( 1 - \frac{\gamma^2}{z_{12}^2} \right) \left( 1 - \frac{1}{\gamma^2 z_{12}^2} \right)}, \quad (3)$$

where  $\gamma = [(\Delta_{13} + \Delta_{23})/\Delta_{12}]$ .  $q_3$  is a double-valued function of  $z_{12}$  with four branch points,  $z_{12} = [(\pm\Delta_{13} \pm \Delta_{23})/\Delta_{12}] = \pm\gamma, \pm(1/\gamma)$ .

Thus, in the first step, the eight Riemann sheets of the complex  $\sqrt{s}$  plane are mapped onto two Riemann sheets of the complex  $z_{12}$  plane with four branch points as shown in Fig. 1.

The second step is to uniformize channel 3. It is known that two Riemann sheets with four branch points are homeomorphic to a torus [4,17]. The map from the former with the coordinate  $v$  to the latter with the coordinate  $u$  is given by an elliptic integral. In particular, when  $v = \pm 1$

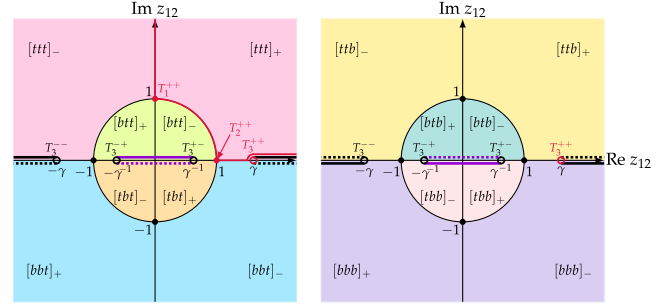


FIG. 1. Two-sheeted complex  $z_{12}$  plane for the three-channel S matrix. Eight Riemann sheets of the complex  $\sqrt{s}$  plane are specified by a set of complex channel momenta, e.g.,  $[ttb]_+$  means  $\text{Im}q_1 > 0, \text{Im}q_2 > 0, \text{Im}q_3 < 0$ , and  $\text{Im}\sqrt{s} > 0$ .  $T_1^{++}, T_2^{++}$ , and  $T_3^{++}$  are physical thresholds of channels 1, 2, and 3, respectively.  $T_3^{++}$  together with its unphysical counterparts,  $T_3^{+-}, T_3^{-+}$ , and  $T_3^{--}$  form the set of branch points.

and  $\pm 1/k$  ( $k \neq 0, \pm 1$ ) are the four branch points, the transformation is given by

$$u = \text{sn}^{-1}(v, k), \quad (4)$$

where  $\text{sn}^{-1}(v, k)$  is the inverse Jacobi’s elliptic function [17,18]

$$\text{sn}^{-1}(v, k) = \int_0^v \frac{ds}{(1-s^2)^{1/2}(1-k^2s^2)^{1/2}}, \quad (5)$$

where also the Riemann sheet on which  $v$  is located has to be specified. Inversely,  $v$  is given as a single-valued function of  $u$  by

$$v = \text{sn}(u, k). \quad (6)$$

Jacobi’s elliptic function is doubly periodic:

$$\text{sn}(u + 2\omega_1, k) = \text{sn}(u + 2\omega_2, k) = \text{sn}(u, k), \quad (7)$$

where

$$2\omega_1 = 4K(k) = 4 \int_0^1 \frac{ds}{\sqrt{(1-s^2)(1-k^2s^2)}},$$

$$2\omega_2 = 2iK'(k) = 2i \int_0^1 \frac{dt}{\sqrt{(1-t^2)(1-(1-k^2)t^2)}}. \quad (8)$$

Therefore, the image of the map, Eq. (4), is a torus with two periods:  $2\omega_1 = 4K(k)$  and  $2\omega_2 = 2iK'(k)$ .

Combining the first and second steps by taking  $k = 1/\gamma^2$ ,  $v = \gamma/z_{12}$ , and  $u = 4K(1/\gamma^2)z$ , we define the three-channel uniformization variable  $z$  as

$$z = \frac{1}{4K(1/\gamma^2)} \operatorname{sn}^{-1}(\gamma/z_{12}, 1/\gamma^2), \quad (9)$$

where  $z_{12}$  is given by Eq. (1). Inversely,  $z_{12}$  is given as a single-valued function of  $z$  by

$$z_{12} = \frac{\gamma}{\operatorname{sn}(4K(1/\gamma^2)z, 1/\gamma^2)}. \quad (10)$$

$q_1$ ,  $q_2$ , and  $q_3$  are given as single-valued functions of  $z$  by

$$\begin{aligned} q_1 &= \frac{\Delta_{12}}{2} \left[ \frac{\gamma}{\operatorname{sn}(4K(1/\gamma^2)z, 1/\gamma^2)} + \frac{\operatorname{sn}(4K(1/\gamma^2)z, 1/\gamma^2)}{\gamma} \right], \\ q_2 &= \frac{\Delta_{12}}{2} \left[ \frac{\gamma}{\operatorname{sn}(4K(1/\gamma^2)z, 1/\gamma^2)} - \frac{\operatorname{sn}(4K(1/\gamma^2)z, 1/\gamma^2)}{\gamma} \right], \\ q_3 &= \frac{\Delta_{12}}{2} \frac{\gamma \operatorname{sn}'(4K(1/\gamma^2)z, 1/\gamma^2)}{\operatorname{sn}(4K(1/\gamma^2)z, 1/\gamma^2)}, \end{aligned} \quad (11)$$

where  $\operatorname{sn}'(u, k) = (d/du)\operatorname{sn}(u, k)$ . By combining the first and second steps, the eight Riemann sheets of the complex  $\sqrt{s}$  plane are mapped onto a torus with periods 1 and  $i\tau$ , where  $\tau = [4K'(1/\gamma^2)/2K(1/\gamma^2)]$ , as shown in Fig. 2 [19].

Next, we investigate the Mittag-Leffler expansion of the three-channel scattering amplitude,  $\mathcal{A}$ , which is related to the S matrix,  $S$ , as  $\mathcal{A}_{ij} = [(S_{ij} - \delta_{ij})/2i\sqrt{k_i k_j}]$ .

The Mittag-Leffler expansion of a meromorphic function on a complex plane,  $\mathcal{F}(z)$ , is given by (see, e.g., [6,7])

$$\begin{aligned} \mathcal{F}(z) &= \sum_i \frac{r_i}{z - z_i} + \text{subtraction terms} \\ &= z^n \sum_i \frac{r_i}{(z - z_i)z_i^n} + \sum_{k=0}^{n-1} \frac{\mathcal{F}^{(k)}(0)}{k!} z^k, \end{aligned} \quad (12)$$

where  $\{z_i\}$  and  $\{r_i\}$  are positions and residues of the poles of  $\mathcal{F}(z)$ . When the sum,  $\sum_i [r_i/(z - z_i)]$ , is divergent, we have to subtract terms of order  $z^k$  ( $k = 0, \dots, n-1$ ) until the  $n$  times subtracted sum,  $z^n \sum_i [r_i/(z - z_i)z_i^n]$ , is convergent. This is exactly the same as in the dispersion theory [7].

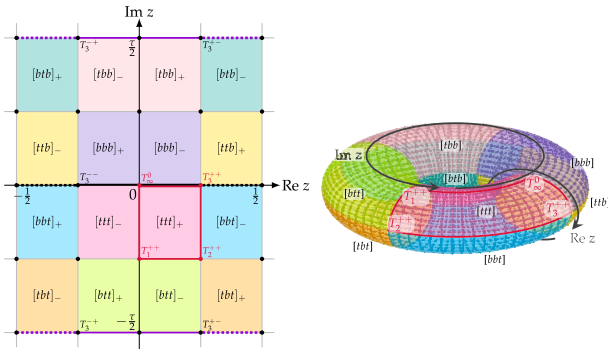


FIG. 2. Torus representation of the three-channel S matrix.

As a function of the uniformization variable,  $z$ , the three-channel scattering amplitude,  $\mathcal{A}(z)$ , is defined on a torus and hence is an elliptic function, a doubly periodic meromorphic function. Therefore, the Mittag-Leffler expansion becomes

$$\begin{aligned} \mathcal{A}(z) &= \sum_i \left( \frac{r_i}{z - z_i} + \sum_{m,n}' \frac{r_i}{z - z_i - \Omega_{m,n}} \right) \\ &\quad + \text{subtraction terms.} \end{aligned} \quad (13)$$

$\sum_i$  is a sum in the fundamental period rectangle,  $\{z_i\}$  and  $\{r_i\}$  are the positions and residues of the poles of  $\mathcal{A}(z)$  in the fundamental period rectangle,  $\sum_{m,n}'$  denotes a sum over all integers  $m$  and  $n$ , excluding  $m = n = 0$ .  $\Omega_{m,n} = 2m\omega_1' + 2n\omega_2'$ . ( $2\omega_1' = 1$  and  $2\omega_2' = i\tau$  for our definition of  $z$ , but what follows holds for arbitrary periods,  $\omega_1'$  and  $\omega_2'$ .) The residues,  $\{r_i\}$ , satisfy the condition  $\sum_i r_i = 0$  [4,17,18]. In the parenthesis of Eq. (13), the first and second terms are called topologically trivial and nontrivial contributions, respectively.

$\sum_{m,n}' [r_i/(z - z_i - \Omega_{m,n})]$  is linearly divergent and  $\mathcal{A}(z)$  is given in the form of Eq. (12) with  $n = 2$ , unless the sum in the fundamental period rectangle causes further divergences. We can rewrite it as

$$\mathcal{A}(z) = \sum_i r_i \zeta(z - z_i) + C_0 + C_1 z, \quad (14)$$

where  $\zeta(z)$  is the Weierstrass zeta function [17,18] defined by

$$\begin{aligned} \zeta(z) &= \frac{1}{z} + \sum_{m,n}' \left( \frac{1}{z - \Omega_{m,n}} + \frac{1}{\Omega_{m,n}} + \frac{z}{\Omega_{m,n}^2} \right) \\ &= \frac{1}{z} + \sum_{m,n}' \frac{z^2}{(z - \Omega_{m,n})\Omega_{m,n}^2}. \end{aligned} \quad (15)$$

The Weierstrass zeta function is odd,  $\zeta(-z) = -\zeta(z)$ , and is quasiperiodic,  $\zeta(z + 2\omega_1) = \zeta(z) + 2\eta_1$  and  $\zeta(z + 2\omega_2) = \zeta(z) + 2\eta_2$ , for constants  $\eta_1$  and  $\eta_2$ .  $C_0$  is determined from the asymptotic condition that the scattering amplitude should vanish as  $s \rightarrow \infty$ , i.e.,  $\mathcal{A}(0) = 0$ , as  $C_0 = -\sum_i r_i \zeta(-z_i) = \sum_i r_i \zeta(z_i)$ , where  $\zeta(-z) = \zeta(z)$  is used.  $C_1$  is determined from the periodicity of  $\mathcal{A}(z)$ , i.e.,  $\mathcal{A}(z + 2\omega_1) = \mathcal{A}(z + 2\omega_2) = \mathcal{A}(z)$  as  $C_1 = 0$ , where  $\sum_i r_i = 0$ ,  $\zeta(z + 2\omega_1) = \zeta(z) + 2\eta_1$  and  $\zeta(z + 2\omega_2) = \zeta(z) + 2\eta_2$  are used. Therefore, we finally obtain

$$\mathcal{A}(z) = \sum_i r_i [\zeta(z - z_i) + \zeta(z_i)], \quad (16)$$

where  $r_i [\zeta(z - z_i) + \zeta(z_i)]$  is identified as the contribution of the  $i$ th pole to the three-channel scattering amplitude,  $\mathcal{A}(z)$ .

Generalized uniformization, Eq. (9), together with Eq. (1), its inverse, Eq. (11), and the Mittag-Leffler expansion, Eq. (16), are the main results of the formal part of this Letter.

If  $z_i$  is a pole of  $\mathcal{A}(z)$  with a residue  $r_i$ , so is  $-z_i^*$  with a residue  $-r_i^*$  because of the unitarity of the  $S$  matrix,  $\mathcal{S}(-q_1^*, -q_2^*, -q_3^*) = \mathcal{S}^*(q_1, q_2, q_3)$  or  $\mathcal{S}(-z^*) = \mathcal{S}^*(z)$ . Therefore, poles appear either as pairs symmetrically with respect to the imaginary  $z$  axis with complex residues related to each other, or independently on the axis,  $\text{Re}z = 0$  or  $0.5$ , with purely imaginary residues.

Now, we examine the above results in a simple model of the  $S = -2$ ,  $I = 0$ ,  $J^P = 0^+$ ,  $\Lambda\Lambda - N\Xi - \Sigma\Sigma$  coupled-channel scattering, in which possible existence of the  $H$  particle [20] has extensively been studied both theoretically and experimentally. Hereafter, channels  $\Lambda\Lambda$ ,  $N\Xi$ , and  $\Sigma\Sigma$  are referred to as 1, 2, and 3, respectively. We generalize a nonrelativistic effective field theory for nucleon scattering [21] to the coupled three-channel scattering. The leading-order effective Lagrangian in the flavor-singlet  ${}^1S_0$  channel is given by

$$\mathcal{L} = B^\dagger \left( i\partial_t + \hat{M} + \frac{\nabla^2}{2\hat{M}} \right) B - \frac{1}{2} [BB]^\dagger \hat{C} [BB], \quad (17)$$

where  $B = (N \Lambda \Sigma \Xi)^T$  and  $[BB] = (\Lambda\Lambda N\Xi \Sigma\Sigma)^T$ . The interaction is assumed to be only in the flavor-singlet channel as

$$\hat{C} = C \begin{pmatrix} \frac{1}{8} & \frac{1}{4} & -\frac{\sqrt{3}}{8} \\ \frac{1}{4} & \frac{1}{2} & -\frac{\sqrt{3}}{4} \\ -\frac{\sqrt{3}}{8} & -\frac{\sqrt{3}}{4} & \frac{3}{8} \end{pmatrix}, \quad (18)$$

where  $C$  is a coupling of dimension  $(\text{mass})^{-2}$ .

The  $3 \times 3$  scattering amplitude,  $\hat{\mathcal{A}}$ , is given by

$$i\hat{\mathcal{A}} = -i\hat{C}(\hat{1} - \hat{G}\hat{C})^{-1}, \quad (19)$$

which is rescaled from the previous definition as  $(4\pi/\sqrt{M_i M_j})\mathcal{A}_{ij} \rightarrow \mathcal{A}_{ij}$ .  $\hat{G}$  is the diagonal  $3 \times 3$  Green function,  $G_{ij} = \delta_{ij}G_i$ ,  $G_i = [(-i\mu_i k_i)/2\pi]$ , and  $\mu_i = [M_i M'_i / (M_i + M'_i)]$  is the reduced mass in the channel,  $i$ . Because the model is nonrelativistic,  $\sqrt{s} = \varepsilon_i + (k_i^2/2\mu_i)$ , and  $k_i = \sqrt{(\mu_i/\varepsilon_i)q_i + O(q_i^3)}$ . The difference of  $k_i$  and  $\sqrt{(\mu_i/\varepsilon_i)q_i}$  can be incorporated but is nonessential in the following discussion, which is ignored just for simplicity. Masses  $M_N, M_\Lambda, M_\Sigma$ , and  $M_\Xi$  are taken to be average masses of charged baryons in review of particle physics [22]. In this model the number of poles is four, which is due to the extremely simple structure of the interaction. This model is used in order to demonstrate validity of our formalism but not to describe realistic physics.

Real and imaginary parts of the  $\Lambda\Lambda \rightarrow \Lambda\Lambda$  elastic scattering amplitude,  $\mathcal{A}_{11}$ , are shown in Fig. 3 for four different cases, (a)–(d), with different coupling,  $C$ , where we present the amplitudes of direct model calculation, reconstructed via the uniformized Mittag-Leffler expansion with all four poles, 1 + 2 + 3 + 4, the contributions from

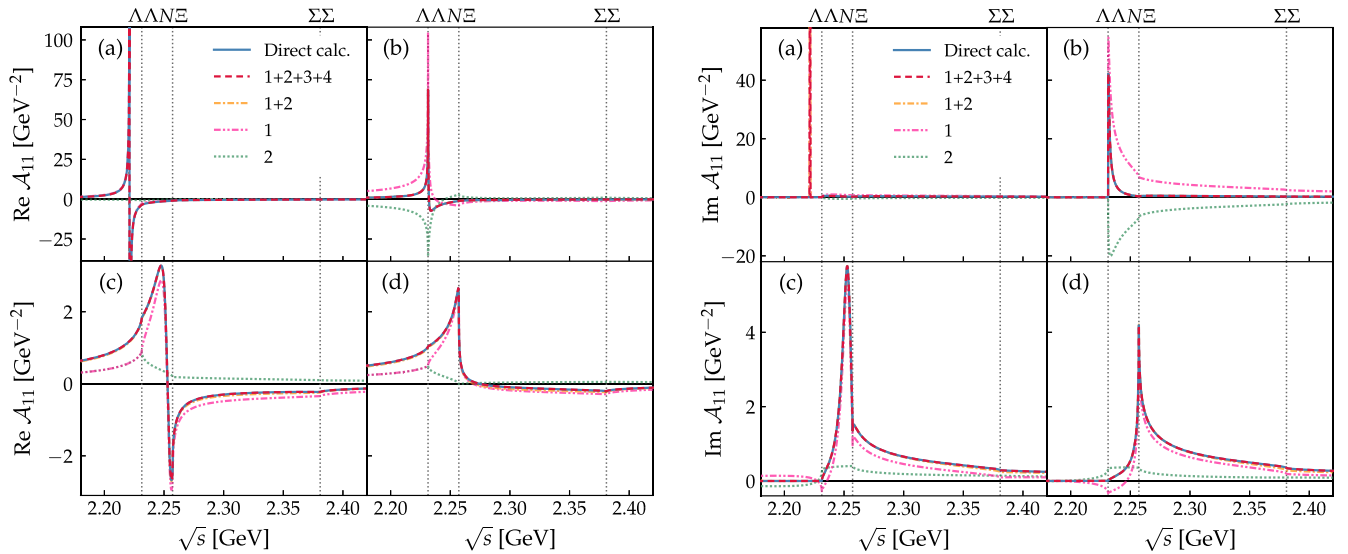


FIG. 3. Real and imaginary parts of the  $\Lambda\Lambda \rightarrow \Lambda\Lambda$  elastic scattering amplitude,  $\mathcal{A}_{11}$ , for cases (a)–(d). Lines represent the amplitude of direct model calculation (blue, solid), reconstructed uniformized Mittag-Leffler expansion with all four poles 1 + 2 + 3 + 4 (red, dashed), contributions from pole 1 (pink, dot-dot-dashed), pole 2 (green, dotted), and their sum 1 + 2 (orange, dot-dashed), respectively.

TABLE I. Pole positions and residues of the  $\Lambda\Lambda \rightarrow \Lambda\Lambda$  elastic scattering amplitude,  $\mathcal{A}_{11}$ , for cases (a)–(d). The first and second rows are the pole positions,  $z_i$ , and residues,  $r_i$ , respectively, on the torus. The third row is the complex center-of-mass energy of the pole,  $\sqrt{s_i}$ , in units of [GeV] and the complex Riemann sheet. The threshold energies,  $\varepsilon_1$ ,  $\varepsilon_2$ , and  $\varepsilon_3$ , are 2.231, 2.257, and 2.381 GeV, respectively.

	$C$ (GeV $^{-2}$ )	Pole 1	Pole 2	Pole 3	Pole 4
(a)	40.00	$-0.267i$ $0.172i$ 2.221 [ttt]	$-0.496i$ $-0.154i$ 2.200 [btt]	$0.5 + 0.043i$ $-0.015i$ $-1.802i$ [ttb]	$0.5 - 0.702i$ $-0.004i$ 13.477i [tbt]
(b)	45.60	$-0.371i$ 1.750i 2.231 [btt]	$-0.398i$ $-1.727i$ 2.229 [btt]	$0.5 + 0.048i$ $-0.018i$ $-1.252i$ [ttb]	$0.5 - 0.700i$ $-0.005i$ 11.722i [tbt]
(c)	60.00	$0.177 - 0.392i$ $-0.215 + 0.018i$ 2.253 $- 0.005i$ [btt]	$-0.177 - 0.392i$ $0.215 + 0.018i$ 2.253 $+ 0.005i$ [btt]	$0.5 + 0.060i$ $-0.027i$ 0.907 [ttb]	$0.5 - 0.697i$ $-0.009i$ 8.657i [tbt]
(d)	80.00	$0.271 - 0.402i$ $-0.249 + 0.028i$ 2.259 $+ 0.002i$ [tbt]	$-0.271 - 0.402i$ $0.249 + 0.028i$ 2.259 $- 0.002i$ [tbt]	$0.5 + 0.073i$ $-0.038i$ 1.510 [ttb]	$0.5 - 0.691i$ $-0.017i$ 6.124i [tbt]

pole 1, 2, and their sum, 1 + 2, respectively. Pole positions and residues of  $\mathcal{A}_{11}$  are given in Table I.

Sharp structures are observed below the  $\Lambda\Lambda$  threshold (bound state) in case (a), at the  $\Lambda\Lambda$  threshold (virtual state) in case (b), between the  $\Lambda\Lambda$  and  $N\Sigma$  threshold (resonance) in case (c), and at the  $N\Sigma$  threshold (“threshold cusp”) in case (d). The amplitudes of direct model calculation and Mittag-Leffler expansion with all four poles, 1 + 2 + 3 + 4, perfectly coincide, which confirms our result, Eq. (16). The contribution from pole 1, which is nearest to the physical domain, gives the sharp structures of the amplitudes of direct model calculation. The sum of contributions from poles 1 and 2 reproduces the amplitudes of direct model calculation in almost the entire physical domain. This is due to the extremely simple nature of the model, i.e., the number of poles is four and only two of them are close to the physical domain, which will not be the case in a more realistic situation.

Figure 4 is the contour plot of  $|\mathcal{A}_{11}|^2$  on the torus, a map of the three-channel S matrix, for cases (a)–(d). It can be observed that as the coupling,  $C$ , increases, pole 1 moves along the imaginary axis transitioning from a bound-state pole on the [ttt] sheet in case (a) to a virtual-state pole on the [btt] sheet in case (b), then it becomes a resonance pole on the [btt] sheet in case (c), and finally a pole on the [tbt] sheet, which causes a “threshold cusp” in case (d). Pole 2 moves along the imaginary axis on the [btt] sheet until it merges with pole 1. Then, it moves symmetrically to pole 1 with respect to the imaginary axis. Poles 3 and 4 hardly move. From Fig. 4 together with Fig. 3, one can clearly observe that the effects of the poles show up as sharp structures on the scattering amplitude around the nearest physical energy region. We would like to mention here that the use of the uniformization variable makes it extremely easy and transparent to locate the positions of poles. When

one traces poles on multisheeted complex  $\sqrt{s}$  plane one has to move around different sheets.

The above demonstration shows that as a function of the uniformization variable the three-channel scattering amplitude is indeed given by the Mittag-Leffler expansion, Eq. (16), and can intuitively be understood from the

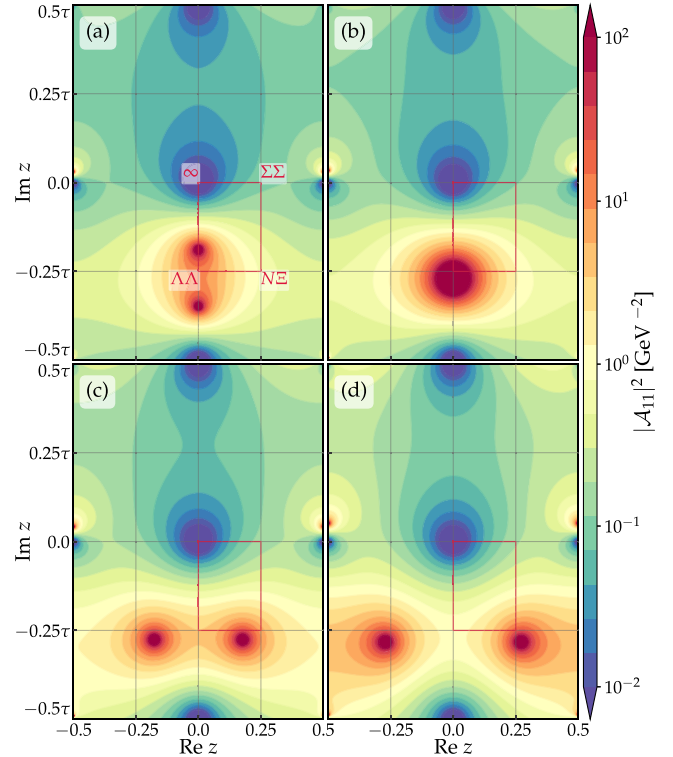


FIG. 4. Contour plot of  $|\mathcal{A}_{11}|^2$  on the torus for cases (a)–(d). The red line corresponds to the physical domain. Labels  $\Lambda\Lambda$ ,  $N\Sigma$ , and  $\Sigma\Sigma$  represent the corresponding thresholds, and  $\infty$  corresponds to infinity point on the physical sheet.



behavior of the poles. Also seen from the above demonstration is that a resonance pole smoothly transitions to a pole, which causes a “threshold cusp,” by the change of the interaction strength. There is no essential difference between these two poles [12].

Having shown that our proposed method is valid, we are now planning to analyze actual experimental data, e.g., [23–25], by our method. We hope that we will report the results of the analysis in the near future.

This work was supported by JSPS KAKENHI Grant No. JP22J15277. We would like to thank Shun’ya Mizoguchi for the instruction on the construction of the Riemann surface. Without his help, the completion of this work would have been much harder. We would also like to thank Akinobu Dote for bringing our attention to the  $H$  particle as a possible application of the 3-channel uniformized Mittag-Leffler expansion. We would also like to thank Koichi Yazaki and the members of the discussion meeting held on the KEK Tokai campus, Yoshinori Akaishi, Toru Harada, Fuminori Sakuma, Shoji Shinmura, and Yasuhiro Yamaguchi.

\*Corresponding author.

wren-phys@g.ecc.u-tokyo.ac.jp

†Corresponding author.

osamu.morimatsu@kek.jp

‡Corresponding author.

tsato@rcnp.osaka-u.ac.jp

- [1] F.-K. Guo, C. Hanhart, Ulf-G. Meissner, Q. Wang, Q. Zhao, and B.-S. Zou, Hadronic molecules, *Rev. Mod. Phys.* **90**, 015004 (2018).
- [2] M. Karliner, J. L. Rosner, and T. Skwarnicki, Multiquark states, *Annu. Rev. Nucl. Part. Sci.* **68**, 17 (2018).
- [3] W. Yamada and O. Morimatsu, New method to extract information of near-threshold resonances: Uniformized Mittag-Leffler expansion of Green’s function and  $T$  matrix, *Phys. Rev. C* **102**, 055201 (2020).
- [4] H. Cohn, *Conformal Mapping on Riemann Surfaces* (Dover Publications, New York, 2010).
- [5] R. G. Newton, *Scattering Theory of Waves and Particles* (Springer, New York, 1982).
- [6] G. Arfken, H. Weber, and F. Harris, *Mathematical Methods for Physicists: A Comprehensive Guide* (Elsevier Science, 2013).
- [7] H. M. Nussenzveig, *Causality and Dispersion Relations* (Academic Press, New York, London, 1972), Vol. 95.
- [8] J. Humblet and L. Rosenfeld, Theory of nuclear reactions: I. resonant states and collision matrix, *Nucl. Phys.* **26**, 529 (1961).
- [9] D. Ramírez Jiménez and N. Kelkar, Different manifestations of S-matrix poles, *Ann. Phys. (Amsterdam)* **396**, 18 (2018).
- [10] M. Kato, Analytical properties of two-channel S-matrix, *Ann. Phys. (N.Y.)* **31**, 130 (1965).
- [11] W. A. Yamada and O. Morimatsu, Application of the uniformized Mittag-Leffler expansion to  $\Lambda(1405)$ , *Phys. Rev. C* **103**, 045201 (2021).
- [12] W. A. Yamada, O. Morimatsu, T. Sato, and K. Yazaki, Near-threshold spectrum from a uniformized Mittag-Leffler expansion: Pole structure of the  $z(3900)$ , *Phys. Rev. D* **105**, 014034 (2022).
- [13] D. Krupa, V. A. Meshcheryakov, and Y. S. Surovtsev, Multichannel approach to studying scalar resonances, *Nuovo Cimento A* **109**, 281 (1996).
- [14] Y. S. Surovtsev, P. Bydzovsky, and V. E. Lyubovitskij, Nature of the scalar-isoscalar mesons in the uniformizing-variable method based on analyticity and unitarity, *Phys. Rev. D* **85**, 036002 (2012).
- [15] W. P. Reinhardt, Fredholm-uniformization computation of elastic scattering amplitudes in the presence of arbitrarily many open channels, *Phys. Rev. A* **8**, 754 (1973).
- [16] H. A. Weidenmüller, Studies of many-channel scattering, *Ann. Phys. (N.Y.)* **28**, 60 (1964).
- [17] T. Takebe, *Daen-sekibun to Daen-Kansuu: Otogi no Kuni no Arukikata (in Japanese)* (Nippon Hyoron Sha Co., Ltd., Tokyo, 2019).
- [18] E. T. Whittaker and G. N. Watson, *A Course of Modern Analysis: An Introduction to the General Theory of Infinite Processes and of Analytic Functions; With an Account of the Principal Transcendental Functions* (Cambridge University Press, Cambridge, 2021).
- [19] See Supplemental Material at <http://link.aps.org/supplemental/10.1103/PhysRevLett.129.192001> for supplemental explanation of the three-channel uniformization.
- [20] R. L. Jaffe, Perhaps a Stable Dihyperon, *Phys. Rev. Lett.* **38**, 195 (1977).
- [21] D. B. Kaplan, M. J. Savage, and M. B. Wise, Nucleon—nucleon scattering from effective field theory, *Nucl. Phys.* **B478**, 629 (1996).
- [22] P. Zyla *et al.* (Particle Data Group), Review of particle physics, *Prog. Theor. Exp. Phys.* **2020**, 083C01 (2020).
- [23] R. Aaij *et al.* (LHCb Collaboration), Observation of  $J/\psi p$  Resonances Consistent with Pentaquark States in  $\Lambda_b^0 \rightarrow J/\psi K^- p$  Decays, *Phys. Rev. Lett.* **115**, 072001 (2015).
- [24] R. Aaij *et al.* (LHCb Collaboration), Observation of a Narrow Pentaquark State,  $P_c(4312)^+$ , and of Two-Peak Structure of the  $P_c(4450)^+$ , *Phys. Rev. Lett.* **122**, 222001 (2019).
- [25] M. Sumihama *et al.* (Belle Collaboration), Observation of  $\Xi(1620)^0$  and Evidence for  $\Xi(1690)^0$  in  $\Xi_c^+ \rightarrow \Xi^- \pi^+ \pi^+$  Decays, *Phys. Rev. Lett.* **122**, 072501 (2019).